DEFINING THE FUNCTIONAL SPACE OF BUS STOPS FROM MLS POINT CLOUDS

S. M. González-Collazo[a], J. Balado[a], E. González[a], H. Lorenzo[a], L. Díaz-Vilariño[a]*

[a]Universidade de Vigo, CINTECX, GeoTECH Group. 36310 Vigo, Spain
(silvgonzalez, jbalado, elena, hlorenzo, lucia)@uvigo.es

Commission IV, WG IV/5

KEYWORDS: Mobile Mapping Systems, LiDAR, Object Classification, 3D Modelling, Space Delimitation, Urban Mobility.

ABSTRACT:
Urban transports are essential for the mobility of citizens, therefore, functional spaces allocated to them should be correctly defined. This research defines the functional spaces for bus stops based on Mobile Laser Scanning (MLS) point clouds. Specifically, three functional spaces are defined; functional space allocated for the marquee (pedestrian space), functional space allocated for the road markings (bus space), and functional space allocated for the bus stop (pedestrians and bus). The method presented is divided into four stages; 1) Bus stop location in the point cloud from given geographical coordinates, 2) Selection of the region of interest (ROI), 3) Classification of the elements in the ROI, 4) Functional space definition. Several algorithms are used to reduce the computational time (point density reduction) and to classify the different elements contained in the bus stop (DBSCAN, height, width, and intensity filter). In addition, bounding boxes are defined to delimit the functional spaces, being compared with the ground truth box. Seven bus stops sited in Palencia (Spain) were analysed. Results show an F1-score value of 0.98 regarding the classification of the elements. Functional spaces allocated for marquees were perfectly defined. Although most of the estimated functional spaces allocated for the bus and the bus stop have high accuracy, in some cases this accuracy decreases due to the functional space allocated for the bus was overestimated.

1. INTRODUCTION

Functional spaces can be explained by several definitions and classified considering different elements. A space can be understood as an area or location with defined boundaries and characteristics for specific uses. Zlatanova et al., (2020) studied the spaces in spatial science and urban applications, reviewing definitions and classifications of space. They concluded that despite the space being discretized in varying manners according to the application, there are still many similarities between the investigated disciplines. Diakité and Zlatanova, (2018) defined a functional space as a subspace allowing to define an area of function necessary to perform specific tasks or to reach and interact with an object, dedicated to a certain activity.

In cities with large extension, urban transport is essential for the mobility of citizens, therefore the functional space allocated to them should be well defined. The approximate location of urban transport stops (bus, metro, tram or taxi), as well as other establishments (supermarkets, restaurants, schools, etc.), can be found in geolocation applications or by consulting the open data of the governmental institutions of each city. Some authors studied the bus arrival time prediction, (Yu et al., 2011), and others analysed routes optimization, (Ibeas et al., 2010; Schittekat et al., 2013). However, few authors have focused on the characterization of bus stops and their functional space. The functional space associated with these elements, especially the open or semi-open spaces, is not properly mapped.

To identify urban elements, numerous authors used Mobile Laser Scanning (MLS) point clouds as input data, (Teo and Chiu, 2015; Yan et al., 2016). This type of data allows obtaining georeferenced information on urban environments and extracting geometric features. Previous studies are mainly based on the characterization of traffic signs, or pole-like elements like traffic lights or trees. Soilán et al., (2016) proposed a method to identify both geometric and semantic properties of traffic signs in urban and highway environments based on MLS point cloud data and RGB imagery. They isolated each traffic sign using a DBSCAN-based clustering, an intensity filter and extracting geometric parameters. Then, based on RGB imagery, they obtained a semantic inventory. Yu et al., (2015) studied the extraction of street light poles from MLS point cloud data. They used Euclidean clustering to group the off-ground points. Then, they applied a Ncut segmentation to split those clusters with more than one object and finally they constructed a pairwise 3D shape context to obtain the light poles. Cabo et al., (2014); Ordóñez et al., (2017) used a voxelization of the MLS point cloud to characterize the pole-like street furniture, and Wu et al., (2013) also applied a voxelization to identify urban vegetation and street trees. Rodríguez-Cuenca et al., (2015) detected and classified pole-like objects based on an anomaly detection algorithm and Aijazi et al., (2014) studied a feature estimation of windows in 3D urban point clouds based on an analysis of variance measurements. ALS data was used by Tran et al., (2018) to obtain a change detection and classification in urban areas based on machine learning.

This study aims to define three types of functional spaces allocated for bus stops. A region of interest (ROI) is selected considering the location of the bus stop. Then the elements within the ROI are classified, focusing on the elements belonging to bus stops (marquees, vertical bus stops, informative panels, road markings and traffic signs). Finally, three functional spaces related to bus stops are defined and identified.

* Corresponding author

This paper is organized as follows. Section 2 presents the proposed method. The results are shown and analysed in Section 3. Finally, Section 4 concludes this work.

2. METHOD

The proposed method is based on four main steps: 1) Bus stop location in the point cloud from given geographical coordinates, 2) Delimitation of the region of interest (ROI), 3) Classification of the elements in the ROI, 4) Functional space definition. Figure 1 shows the workflow of the method.

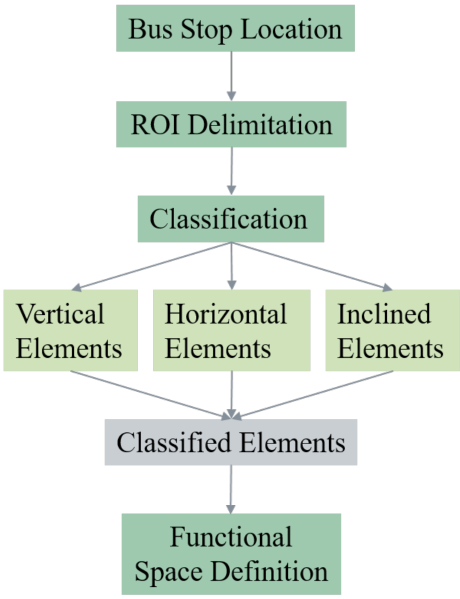

Figure 1. Workflow

2.1 Bus stop location and ROI delimitation

First, the locations of the bus stops are searched within the MLS point clouds. The locations of the bus stops are taken from the open data source of the city or OpenStreetMaps. Based on these data, the closest point to the bus stop location in the point cloud is selected. From the previous point, a $20\ m$ radius search is conducted to define the ROI. Then, the ROI is rotated to align the side where the bus stop is located with the XZ plane. A point density reduction is applied to reduce the computational time of further processes. Figure 2 shows the workflow of these two stages.

2.2 ROI classification

The classification is performed in two steps. First, the points of the ROI are classified into vertical elements, horizontal elements and inclined elements, and noise points are defined. For this purpose, tilt $I(Ix, Iy)$ and curvature C are calculated from the normal surfaces of each point concerning its k nearest neighbours. The ground inclination Ig is also obtained based on the trajectory vectors. The curvature threshold is defined by a range between [5,20] and the inclination threshold is defined with a value of 0.03. The following conditions are defined to classify the elements in the different categories:

- Vertical elements: $(Ix \,\&\, Iy) \geq 20$
- Horizontal elements: $Ix < (5 + Ig) \,\&\, Iy < 5$
- Inclined elements: $5 < (Ix \,\&\, Iy) < 20 \,\&\, C < 0.03$

Then, a second classification is done to identify the objects inside horizontal, inclined, and vertical elements. Horizontal elements are classified into sidewalk and road. This classification is based on the DBSCAN algorithm, (Wang et al., 2019), which groups the points in clusters based on a minimum distance eps and a minimum number of neighbours $Nmin$. The parameters used in the DBSCAN algorithm to group the points of the horizontal elements in clusters are; $eps = 0.1\ m$ and $Nmin = 10$. To classify clusters on roads and sidewalks, the distance Dc and the height Hc of the cluster are considered. Clusters are considered near to the ground if Hc is smaller than the ground height Hg plus a height threshold Ht (equal to $0.3\ m$). In addition, a distance threshold Dt equal to $0.1\ m$ within the cluster is considered. Clusters are classified as road if they are near the ground and Dc is smaller than $0.1\ m$. If Dc is greater than $0.1\ m$ and the cluster is near the ground, is classified as the sidewalk. Clusters that do not fulfil the parameters to be sidewalk or road are classified as other horizontal elements. Also, road markings related to bus stops are searched within the points classified as a road, based on DBSCAN ($eps = 0.4\ m$ and $Nmin = 20$) and intensity values ($Intensity > 1000$). Inclined elements are classified into ramps or no ramps using the DBSCAN algorithm, ($eps = 0.1\ m$ and $Nmin = 10$). Figure 3 is presented a workflow of horizontal and inclined elements classification.

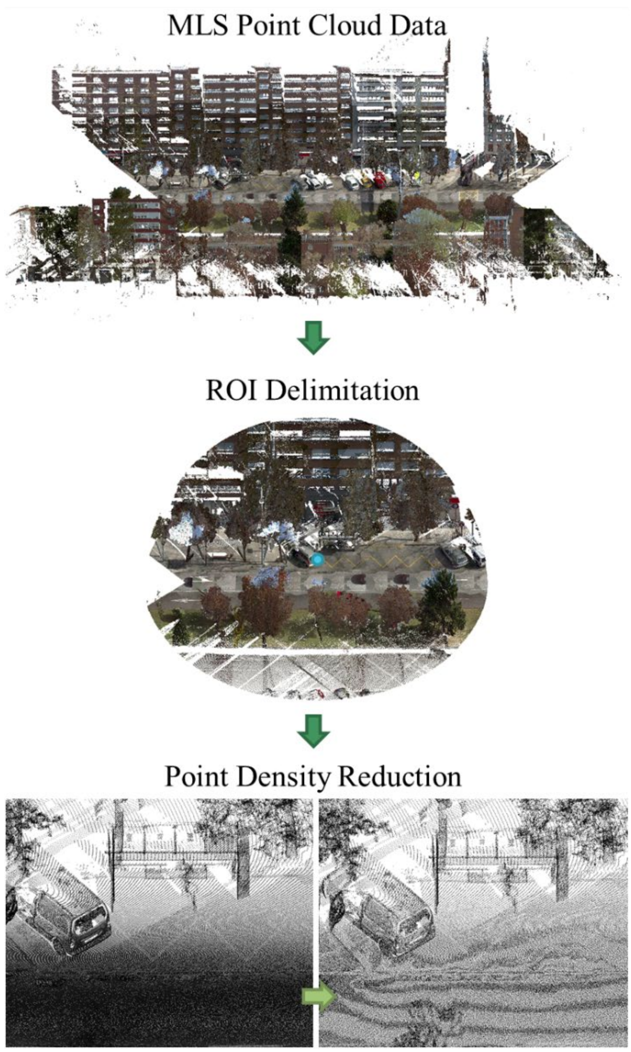

Figure 2. Workflow of the initial MLS point cloud processing. The blue dot indicates the centre of the ROI

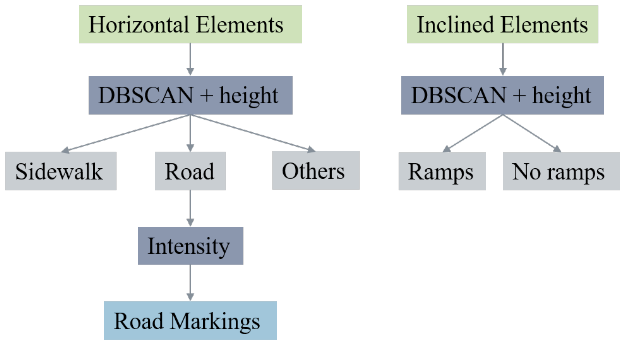

Figure 3. Horizontal and inclined elements classification

Vertical elements are classified into marquees, vertical bus stops, informative panels, traffic signs and other vertical elements, (Figure 4). This classification is done by applying rasterization ($grid = 0.1\,m$) to the point cloud containing the vertical elements. Based on the obtained raster and the heights, vertical elements are first classified into steps and elements different from steps. The height variance and the difference between the pixel height Hp and the ground height Hg are analyzed in each pixel. Pixels are classified as steps if the height variance is within a threshold of $[0.015\,m, 0.2\,m]$ and the difference between Hp and Hg is less than $0.3\,m$. Otherwise, pixels are classified as elements different from steps. This second group is again classified using a DBSCAN ($eps = 0.1\,m$ and $Nmin = 10$). In this stage, only the vertical elements located in the same space as the sidewalk (regarding the side of the bus stop) are considered. The obtained clusters are classified depending on their height, width, and intensity. If the intensity of the cluster is higher than a specific value and Hc is between $2\,m$ and $3.2\,m$, then this cluster is classified as a traffic sign. In case the intensity is not higher than the specific value, the clusters are classified into a bus stop, marquees and informative posts depending on their height and width, according to the parameters shown in Table 1.

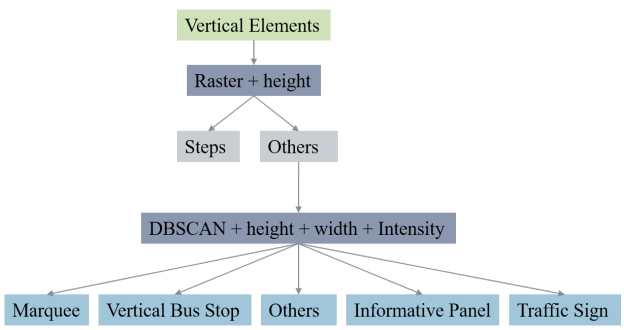

Figure 4. Vertical elements classification

Vertical Element	Height	Width	Intensity
Marquee	2-3.2 m	> 3 m	< 1000
Vertical Bus Stop	2-3.2 m	< 0.3 m	< 1000
Informative Panel	2-3.2 m	0.3-0.75 m	< 1000
Traffic Sign	2-3.2 m	-	> 1000

Table 1. Height, width, and intensity filter parameters

Figure 5 shows the ROI of a specific bus stop, with the classified elements. Finally, the classified points are re-rotated to their original positions.

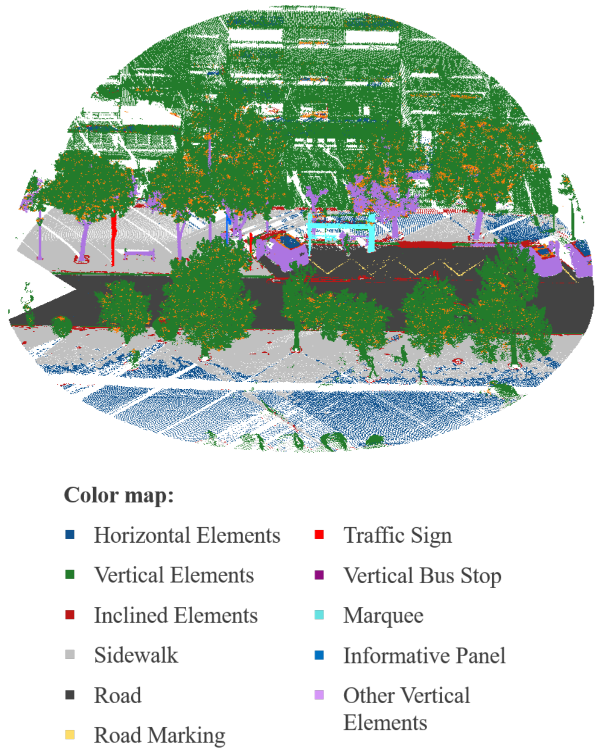

Figure 5. ROI of a bus stop with classified elements

2.3 Functional Space Definition

Once the elements within the ROI are classified, three functional spaces are defined:

- Functional space allocated for marquees (*Pedestrian space*)
- Functional space allocated for road markings (*Bus space*)
- Functional space allocated for the bus stop (*Pedestrian & bus space*)

Oriented bounding boxes, (Wang et al., 2021), are estimated and used to delineate the different functional spaces. The *Pedestrian space* is defined by the marquee itself, (Figure 6a). The *Bus space* is defined by the road markings, (Figure 6b), and the *Pedestrian & bus space* is defined by the vertical bus stop or marquee, the informative panel, if that is the case, and the road marking, (Figure 6c).

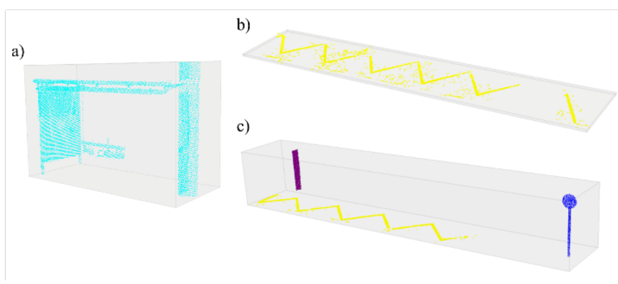

Figure 6. Functional space definition: a) *Pedestrian space*, b) *Bus space*, c) *Pedestrian & bus space*

3. EXPERIMENTS AND RESULTS

3.1 Data

The proposed method was tested in seven bus stops sited in different streets located in Palencia (Spain). The input data were MLS point clouds of the streets, with 12.6 million points each of them, (Figure 7). MLS point clouds were acquired with the LYNX Mobile Mapper of Optech.

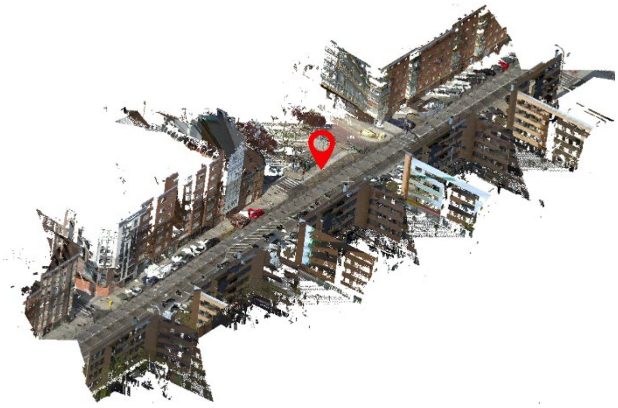

Figure 7. MLS point cloud of one street containing a bus stop (red mark)

3.2 Results

Figure 8 shows the results obtained in the seven bus stops analyzed. Bus stop A is sited in Don Sancho street, bus stop B is in San Antonio square, bus stops C and D are in Paseo de la Julia, bus stops E and F are in Modesto Lafuente avenue and bus stop G is in Manuel Rivera avenue. Almost all the searched elements were correctly classified. In bus stops B and E, one traffic sign was wrongly classified as an informative panel. This is because these clusters fulfilled with the height of a traffic sign but they did not have enough intensity value to be classified as a traffic sign.

Road markings were well estimated, although some of them (bus stop A and bus stop D) were overestimated because there were other road markings in the close surroundings of the bus stop.

To analyze the quality of the results, several metrics were used and contrasted with manual ground truth. Table 2 shows a confusion matrix of the obtained results. All the elements were correctly classified except for two traffic signs, which were confused with informative panels.

		Predicted value				
		Marquee	Vertical Bus Stop	Informative panel	Traffic Sign	Road Marking
Real Value	Marquee	2	0	0	0	0
	Vertical Bus Stop	0	6	0	0	0
	Informative panel	0	0	3	2	0
	Traffic Sign	0	0	0	8	0
	Road Marking	0	0	0	0	8

Table 2. Confusion matrix

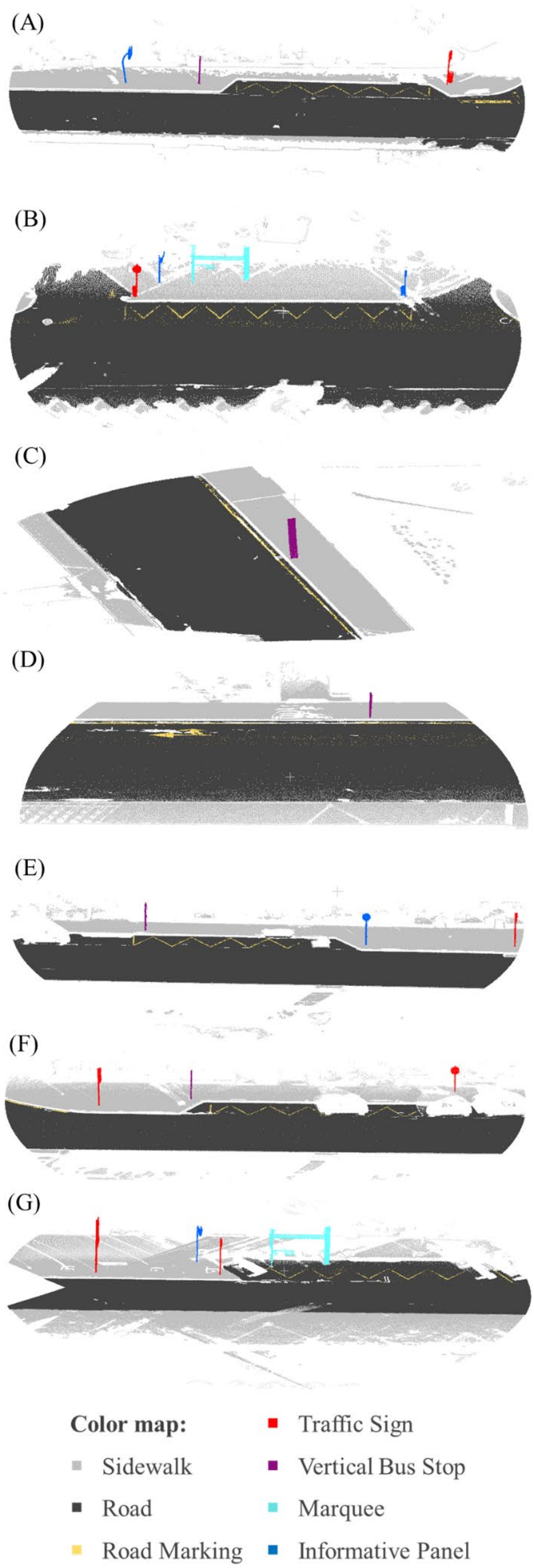

Figure 8. Bus stops with the elements classified

An F1-score value of 0.9796 was obtained according to Equation 1, being P the precision and R the recall. Regarding the functional spaces, the intersection over union (IoU) (Equation 2) was used to measure how similar the predicted bounding box and ground truth box are, being A_o the overlap area and A_u the union area.

$$F1_{score} = \frac{2 \times P \times R}{P + R} \quad (1)$$

$$IoU = \frac{A_o}{A_u} \quad (2)$$

Table 3 shows these measures regarding the XY plane and the XZ plane of the three defined functional spaces in each one of the seven bus stops.

	***IoU* (XY)**		
Bus stop	*Pedestrian space*	*Bus space*	*Pedestrian & bus space*
A	-	0.44	0.52
B	1.00	0.33	0.53
C	-	1.00	1.00
D	-	0.18	0.29
E	-	1.00	1.00
F	-	0.41	0.55
G	1.00	1.00	1.00
	***IoU* (XZ)**		
Bus stop	*Pedestrian space*	*Bus space*	*Pedestrian & bus space*
A	-	0.29	0.77
B	1.00	0.41	0.58
C	-	1.00	1.00
D	-	0.53	0.92
E	-	1.00	1.00
F	-	0.41	0.55
G	1.00	1.00	1.00

Table 3. Intersection over Union (***IoU***)

The functional spaces of bus stop C, E and G were predicted with an accuracy of 100% concerning the ground truth. The *Pedestrian space* in bus stop B was perfectly estimated while the *Bus space* and the *Pedestrian & bus space* was overestimated because some road markings near the specific bus stop road markings were detected and classified inside the *Bus space*. The *Pedestrian & bus space* contain the road markings; therefore, this functional space was also overestimated. The functional spaces of the bus stop D were overestimated considering the XY plane. Regarding the XZ plane, the functional spaces belonging to bus stop D were estimated with higher accuracy. Functional spaces of bus stop A and F were also overestimated, due to the road markings, (Figure 10).
However, it can be said that most of the functional spaces were estimated with high accuracy in both planes. The average value obtained with the IoU metric for the *Pedestrian space* is 1 in the XY plane and XZ plane. The average value for the *Bus space* is 0.65 in both planes and the average value for the *Pedestrian & bus space* is 0.7 in the XY plane and 0.85 in the XZ plane.

Figure 10 shows the functional space allocated for a marquee of bus stop B, and consequently the *Pedestrian space*. Figure 11 shows the *Pedestrian & bus space* of bus stop C, which was composed of a vertical bus stop and a line road marking. The *Pedestrian & bus space* of the bus stop G is represented in Figure 12. Bus stop G is composed of a marquee, an informative panel and a zigzag road marking.

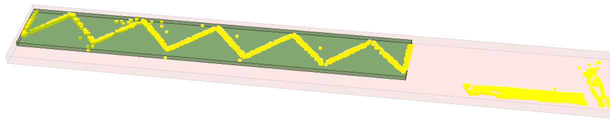

Figure 9. *Bus space* (bus stop A). Ground truth box (green square), estimated box (red square)

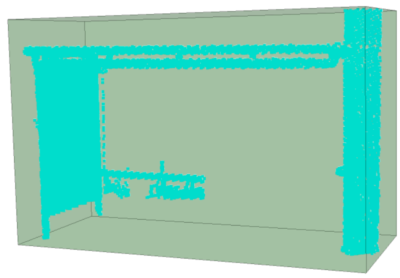

Figure 10. *Pedestrian space* (bus stop B). The estimated box is coincident with the ground truth.

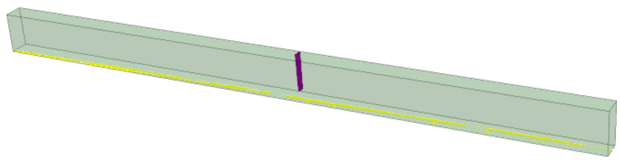

Figure 11. *Pedestrian & bus space* allocated for bus stop C. The estimated box is coincident with the ground truth.

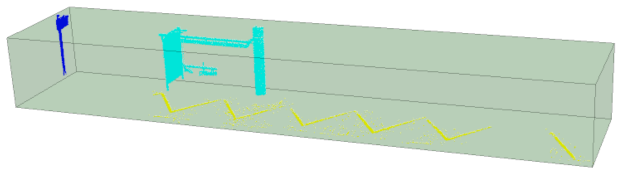

Figure 12. *Pedestrian & bus space* allocated for bus stop G. The estimated box is coincident with the ground truth.

4. CONCLUSIONS

Defining the functional spaces of bus stops allows to identify the area allocated to public transport within a city. With the proposed method the functional spaces allocated to bus stops are defined. Three different scenarios are presented, the functional space allocated to the marquee (*Pedestrian space*), the functional space allocated to the bus (*Bus space*) and the total functional space of the bus stop (*Pedestrian & bus space*). The results show that almost all the searched elements are correctly identified. Only two traffic signs were misclassified as informative panels. Both the precision and recall have high values in all the types of elements classified, which leads to a 0.98 value of the F1-sore metric. In addition, a comparison of the predicted functional space and the ground truth functional space is done. At some bus stops the *Bus space* is overestimated and, as a consequence, the *Pedestrian & bus space*. Despite the points being correctly defined because they are road markings, they do not belong to the specific road markings of the bus stop. The *Pedestrian space* is identified with precise accuracy, as well as the majority of the *Pedestrian & bus spaces*. The overall values obtained with the *IoU* metric are between 0.65 and 1. Therefore, with the proposed method is possible to correctly define the functional space of bus stops.

In future work, other elements in the near surroundings of the bus stops can be defined, especially the ones which facilitate the use of bus stops, like benches. A reconstruction of the pedestrian occluded areas can be done. In addition, more case studies can be analyzed, studying other types of bus stops configurations and the functional spaces allocated to them.

ACKNOWLEDGMENTS

This research was funded by the Xunta de Galicia, grant numbers ED481B-2019-061 and ED431C 2020/01, and by the Government of Spain through project PID2019-105221RB-C43 funded by MCIN/AEI/10.13039/501100011033, through project PDC2021-121239-C32 funded by MCIN/AEI/10.13039/ 501100011033 and "NextGenerationEU"/PRTR and through human resources grant RYC2020-029193-I funded by MCIN/AEI/ 10.13039/501100011033 y FSE \"El FSE invierte en tu futuro”. It reflects only the authors’ views.

REFERENCES

Aijazi, A.K., Checchin, P., Trassoudaine, L., 2014. Automatic detection and feature estimation of windows in 3D urban point clouds exploiting façade symmetry and temporal correspondences. *Int. J. Remote Sens.* 35, 7726–7748. https://doi.org/10.1080/01431161.2014.975420

Balado, J., Díaz-Vilariño, L., Arias, P., Soilán, M., 2017. Automatic building accessibility diagnosis from point clouds. *Autom. Constr.* 82, 103–111. https://doi.org/https://doi.org/10.1016/j.autcon.2017.06.026

Cabo, C., Ordoñez, C., García-Cortés, S., Martínez, J., 2014. An algorithm for automatic detection of pole-like street furniture objects from Mobile Laser Scanner point clouds. ISPRS J. Photogramm. *Remote Sens.* 87, 47–56. https://doi.org/https://doi.org/10.1016/j.isprsjprs.2013.10.008

Diakité, A.A., Zlatanova, S., 2018. Spatial subdivision of complex indoor environments for 3D indoor navigation. *Int. J. Geogr. Inf. Sci.* 32, 213–235. https://doi.org/10.1080/13658816.2017.1376066

Ibeas, Á., dell’Olio, L., Alonso, B., Sainz, O., 2010. Optimizing bus stop spacing in urban areas. Transp. Res. Part E Logist. *Transp. Rev.* 46, 446–458. https://doi.org/https://doi.org/10.1016/j.tre.2009.11.001

Ordóñez, C, Cabo, C., Sanz-Ablanedo, E., 2017. Automatic Detection and Classification of Pole-Like Objects for Urban Cartography Using Mobile Laser Scanning Data. *Sensors* 17. https://doi.org/10.3390/s17071465

Rodríguez-Cuenca, B., García-Cortés, S., Ordóñez, C., Alonso, M.C., 2015. Automatic Detection and Classification of Pole-Like Objects in Urban Point Cloud Data Using an Anomaly Detection Algorithm. *Remote Sens.* 7, 12680–12703. https://doi.org/10.3390/rs71012680

Schittekat, P., Kinable, J., Sörensen, K., Sevaux, M., Spieksma, F., Springael, J., 2013. A metaheuristic for the school bus routing problem with bus stop selection. *Eur. J. Oper. Res.* 229, 518–528. https://doi.org/https://doi.org/10.1016/j.ejor.2013.02.025

Soilán, M., Riveiro, B., Martínez-Sánchez, J., Arias, P., 2016. Traffic sign detection in MLS acquired point clouds for geometric and image-based semantic inventory. ISPRS J. Photogramm. *Remote Sens.* 114, 92–101. https://doi.org/https://doi.org/10.1016/j.isprsjprs.2016.01.019

Teo, T.-A., Chiu, C.-M., 2015. Pole-Like Road Object Detection From Mobile Lidar System Using a Coarse-to-Fine Approach. *IEEE J. Sel. Top. Appl. Earth Obs. Remote Sens.* 8, 1–14. https://doi.org/10.1109/JSTARS.2015.2467160

Tran, T.H.G., Ressl, C., Pfeifer, N., 2018. Integrated Change Detection and Classification in Urban Areas Based on Airborne Laser Scanning Point Clouds. *Sensors* 18. https://doi.org/10.3390/s18020448

Wang, C., Ji, M., Wang, J., Wen, W., Li, T., Sun, Y., 2019. An Improved DBSCAN Method for LiDAR Data Segmentation with Automatic Eps Estimation. *Sensors* 19. https://doi.org/10.3390/s19010172

Wang, Q., Chen, J., Deng, J., Zhang, X., 2021. 3D-CenterNet: 3D object detection network for point clouds with center estimation priority. *Pattern Recognit.* 115, 107884. https://doi.org/https://doi.org/10.1016/j.patcog.2021.107884

Wu, B., Yu, B., Yue, W., Shu, S., Tan, W., Hu, C., Huang, Y., Wu, J., Liu, H., 2013. A Voxel-Based Method for Automated Identification and Morphological Parameters Estimation of Individual Street Trees from Mobile Laser Scanning Data. *Remote Sens.* 5, 584–611. https://doi.org/10.3390/rs5020584

Yan, W.Y., Morsy, S., Shaker, A., Tulloch, M., 2016. Automatic extraction of highway light poles and towers from mobile LiDAR data. *Opt. Laser Technol.* 77, 162–168. https://doi.org/https://doi.org/10.1016/j.optlastec.2015.09.017

Yu, B., Lam, W.H.K., Tam, M.L., 2011. Bus arrival time prediction at bus stop with multiple routes. *Transp. Res. Part C Emerg. Technol.* 19, 1157–1170. https://doi.org/https://doi.org/10.1016/j.trc.2011.01.003

Yu, Y., Li, J., Guan, H., Wang, C., Yu, J., 2015. Semiautomated Extraction of Street Light Poles From Mobile LiDAR Point-Clouds. IEEE Trans. Geosci. *Remote Sens.* 53, 1374–1386. https://doi.org/10.1109/TGRS.2014.2338915

Zlatanova, S., Yan, J., Wang, Y., Diakité, A., Isikdag, U., Sithole, G., Barton, J., 2020. Spaces in Spatial Science and Urban Applications—State of the Art Review. *ISPRS Int. J. Geo-Information* 9. https://doi.org/10.3390/ijgi9010058